Article:
Jones, S.A. and Tomlinson, R.A. (2015) Investigating mixed-mode (I/II) fracture in epoxies using digital image correlation: Composite G(IIc) performance from resin measurements. Engineering Fracture Mechanics, 149. pp. 368-374. ISSN: 0013-7944

https://doi.org/10.1016/j.engfracmech.2015.08.041

Investigating mixed-mode (I/II) fracture in epoxies using digital image correlation: Composite G_{IIc} performance from resin measurements.

Authors: Stephen A. Jones [a], Rachel A. Tomlinson [a,*]

[a] Department of Mechanical Engineering, The University of Sheffield, Sheffield, United Kingdom

*email address r.a.tomlinson@sheffield.ac.uk

Abstract

The digital image correlation technique is applied to investigate mixed-mode (I/II) fracture in five aerospace epoxy formulations, four of which are experimentally toughened. Stress intensity factors are extracted from displacement fields using the Williams method for a range of mode mixities. From these measurements, values of an effective resin K_{IIc} are deduced and these are shown to have a statistically significant relationship with measured composite G_{IIc} mode II toughness values. The differences in constraint between composite and bulk resin specimens are discussed.

Keywords

Mixed-mode, stress intensity factors, epoxy, digital image correlation,

Nomenclature

a	Crack length, mm
c	Critical value
T	T-stress, MPa
G	Energy release rate
K	Stress intensity factor, MPa$\sqrt{m}$
Q	Load at failure, N
r	Radius (polar coordinates from crack-tip), mm
s	Sample standard deviation
θ	Angle (polar coordinates from crack-tip), °

Introduction

The long-term damage tolerance of composite aerospace structures is of obvious importance to airframe designers using these materials, and consequently any new composite material for consideration for primary-structure aerospace application must meet a wide range of minimum mechanical properties, including mode I and II toughness and compressive-strength after sustaining a set energy impact.

Current aerospace composite materials for primary structure application are mostly interlaminar toughened, including primary structures of the Boeing 787 and the Airbus A350-XWB. Interlaminar particle toughening provides cost-effective improvement to toughness and damage tolerance without compromising stiffness or causing significant detriment to solvent resistance performance.

Whilst increasing the intrinsic toughness of a resin generally increases both mode I and mode II toughness [1], the addition of interlaminar toughening particles introduces a variety of possible competing toughening mechanisms. Whilst some particles offer high levels of mode I and mode II toughness, others provide high mode I toughness, but disappointing levels of mode II toughness due to these particles causing cracks to divert straight into the fibre-bed, away from the tough interlaminar region.

In order to formulate new materials for aerospace applications, in a timely and cost-effective way, it is of great benefit if formulations can be screened in as quick and as fundamental a form as possible, with minimum resources. For many years, composite 'systems' have been developed using much testing at a resin-only level; clearly advantageous when one considers the resources required to produce a quality prepreg using an in-development resin formulation. With the advent of third generation prepreg materials, with various exotic structures in the interlaminar region [2], developing formulations becomes ever more time-consuming. Limiting ourselves to the scope of particle toughening, there are countless micron scale thermoplastic, elastomer, inorganic etc. particles that are commercially available, and unlimited scope for engineering new particles.

The bulk resin mode I fracture toughness of novel resin and resin-particle formulations is routinely measured using compact tension (CT) specimens. In the pure mode I case, it is well known that in general, improvement in mode I matrix toughness corresponds to an improvement in composite mode I toughness [1,3,4]. Due to the constrained length-scale in which crack tip yielding can occur, large increases in resin toughness generally result in smaller improvements in composite G_{Ic}. The resin mode I toughness generally bears little connection to composite mode II performance and no suitable method of measuring mode II fracture toughness of the matrix material has previously been identified [1]. So-called pure mode II toughness tests in polymeric materials struggle to apply a consistent shear force to the pre-crack tip; small differences in starter crack angle make a significant difference in applied K_{II}/K_I, which makes a global load-based method prone to large variation.

Traditional mechanics assumes that if cracks grow between the plies in a laminar composite, in the direction of a shear load, then shear failure must occur. However, it is widely acknowledged that the concept of 'interlaminar shear fracture' is not true shear failure; at a material mechanistic level failure can be seen to be tensile-opening in nature [5][1]. Bonds are not seen to break by sliding mechanisms but instead shear hackles are seen on fracture surfaces, the 45° shape of which denotes

failure in the tensile direction at a material level. Thus, micro-mechanically, interlaminar shear failure in composites is somewhat of a misnomer.

To measure true K_{IIc} or G_{IIc}, the failure mode of the specimen must be mode II which leads back to the requirement to constrain crack-path by some method such as the addition of deep grooves to a test specimen, as employed in a study by Ramsteiner [6]. A study by Carpinteri *et al.* [7] into the effect the size of an interlaminar-toughening 'aggregate' had on G_{IIc} found no evidence for the existence of a mode II toughness parameter affecting the (kinked) fracture of their specimens. A similar critique of G_{IIc} tests for composites was made by O'Brien [8] showing that the sliding shear mechanisms assumed by the fracture mechanics definitions of mode II failure do not occur. Instead tensile failures in the matrix occur under critical shear loading.

However, the resistances of both laminar composite and bulk polymer to fracture under shear loading are physical characteristics of great significance to the composite and aerospace industries; pre-cracked composite specimens loaded under shear do fail in the shear direction and have a quantifiable resistance to this crack growth. Composite *'G_{IIc}'* has been shown to be strongly related to damage tolerance and compression after impact behaviour [9,2]. Therefore, for a focused effort in improving interlaminar shear toughness in composites it is important to understand the mechanistic behaviour of the matrix material involved. This paper focuses on the observation of mixed-mode fracture behaviour in aerospace epoxies in order to better understand their behaviour in both bulk resin form and ultimately in aerospace composite components.

Digital Image Correlation (DIC) is a convenient tool for determining displacement fields around crack tips. It is a robust, non-contact, commercially available strain and displacement field measuring tool with growing use in industrial as well as academic research. Greyscale digital images of a randomly patterned specimen surface are recorded and compared with an initial image of the strain-free specimen. Comparison occurs through cross-correlation algorithm performed on 'integration windows' of pixels, usually 15-80 pixels square. Subpixel accuracy is obtained by fitting interpolation functions through the greyscale levels of each integration window. Random patterns are most often applied using matt black paint speckles on a matt white basecoat. A comprehensive examination of the DIC technique can be found in the book by Sutton *et al.* [10].

From the displacement fields, fracture parameters may be extracted and used to quantify and understand fracture behaviour. Whilst photoelasticity is often used for such applications, the formulations under study here are not suited to this technique due to relatively low levels of transparency. Much work has been carried out on the extraction of fracture parameters from (usually DIC) displacement data [11,12,13,14]. This extraction typically involves iteratively mapping displacement field data into either the Williams' stress field solution [15] (equations 1) or through the Muskhelishvili approach detailed in [16, 17].

$$\sigma_{xx} = \frac{K_I}{\sqrt{2\pi r}}\cos\frac{\theta}{2}\left(1 - \sin\frac{\theta}{2}\sin\frac{3\theta}{2}\right) + T + A\sqrt{r}\cos\frac{\theta}{2}\left(1 + \sin^2\frac{\theta}{2}\right) + O(r)$$

$$\sigma_{yy} = \frac{K_I}{\sqrt{2\pi r}}\cos\frac{\theta}{2}\left(1 - \sin\frac{\theta}{2}\sin\frac{3\theta}{2}\right) + A\sqrt{r}\cos\frac{\theta}{2}\left(1 - \sin^2\frac{\theta}{2}\right) + O\left(r^{3/2}\right) \qquad (1a)$$

$$\tau_{xy} = \frac{K_I}{\sqrt{2\pi r}}\cos\frac{\theta}{2}\sin\frac{\theta}{2}\cos\frac{3\theta}{2} - A\sqrt{r}\sin\frac{\theta}{2}\cos^2\frac{\theta}{2} + O(r)$$

$$\sigma_{xx} = \frac{-K_{II}}{\sqrt{2\pi r}}\sin\frac{\theta}{2}\left(2 + \cos\frac{\theta}{2}\cos\frac{3\theta}{2}\right) + B\sqrt{r}\sin\frac{\theta}{2}\left(2 + \cos^2\frac{\theta}{2}\right) + O(r)$$

$$\sigma_{yy} = \frac{K_{II}}{\sqrt{2\pi r}}\sin\frac{\theta}{2}\cos\frac{\theta}{2}\cos\frac{3\theta}{2} - B\sqrt{r}\sin\frac{\theta}{2}\cos^2\frac{\theta}{2} + O\left(r^{3/2}\right) \quad (1b)$$

$$\tau_{xy} = \frac{K_{II}}{\sqrt{2\pi r}}\cos\frac{\theta}{2}\left(1 - \sin\frac{\theta}{2}\sin\frac{3\theta}{2}\right) + B\sqrt{r}\cos\frac{\theta}{2}\left(1 + \sin\frac{\theta}{2}\sin\frac{3\theta}{2}\right) + O\left(r^{3/2}\right)$$

A number of studies [11, 18] have highlighted the importance of the accuracy of the defined crack-tip location for DIC fracture parameter extraction using the Williams method; the papers referenced here both incorporating crack-tip locating algorithms to determine crack-tip location from the displacement field. An alternative method was presented by López-Crespo *et al.* [16] using the Muskhelishvili method, combined with the Sobel edge-finding algorithm, to fracture problems with tough materials and large displacement.

Materials and methods

Five different epoxy formulations; a base control resin A, and four experimentally toughened resins B, C, D and E, were supplied by an industrial partner and tested. Materials were toughened with experimental particulate 'fillers', candidates for aerospace interlaminar toughening agents. The nature of these materials is commercially sensitive and as such some results have been normalised and details of the formulations have not been disclosed.

The epoxy formulations were machined into a specimen geometry based on the work by Arcan and Banks-Sills [19]. These allow mixed-mode loading from pure mode I, to almost pure mode II, performed at 15° loading intervals. Arcan-type specimens were chosen for their material efficiency and low crack-tip rigid body displacement to aid DIC measurement. Whilst not a fracture investigation, the study by Taher *et al.* investigated the shear/tensile behaviour of foam specimens with DIC using an Arcan-type arrangement [20]. For the pure shear arrangement the DIC results clearly showed a uniform shear strain across the specimen ligand. The study used a modified Arcan arrangement to allow variable ratios of compression/shear to be tested in addition to tension/shear. A specimen in the loading grips is shown in figure 1. Since toughness values were to be measured, sharp, naturally propagated cracks were generated by razor-tapping, and so a specimen with an edge-crack was necessary to enable this. Specimens are asymmetrical (notch on one side, machined

out on other side) to ease specimen preparation. Tests were performed at room-temperature, ambient humidity conditions.

A random speckle pattern of black paint on a white background was applied to the specimens using an airbrush. This gave speckle sizes of around 20-50 µm in diameter (equivalent to 4-10 pixels on the camera CCD).

A 2.0MP, 14bit LaVision 2D-DIC camera system was used with a Navitar PreciseEye long-field microscope lens, giving a field of view of 6.0 × 4.5 mm. The camera was fixed at an angle normal to the specimen, and rotated about the z-axis (out-of-plane) to be square to the crack. Cold, fibre-optic LED lighting was used. This arrangement is shown in figure 1.

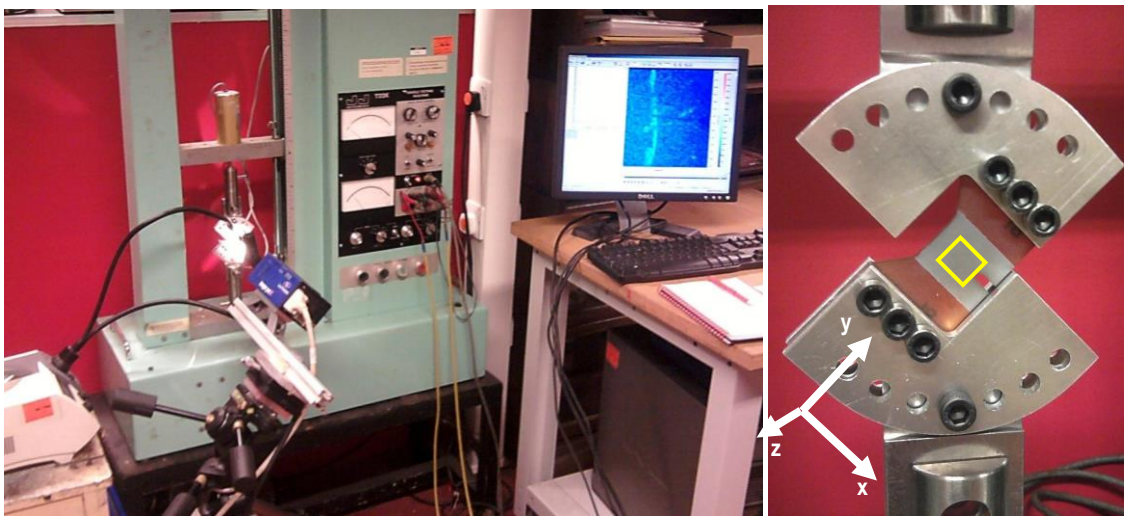

Figure 1 Experimental arrangement. Enlarged is a specimen in grips at a 45° loading angle. DIC field of view (yellow) and coordinate system are overlaid.

LaVision Strainmaster 7.1 was used to determine displacement fields using multi-pass integration windows of size 64x64 pixels, trading some spatial resolution for absolute accuracy. These settings were determined through convergence study. DICITAC (**D**igital **I**mage **C**orrelation **I**ntensity factor and **T**-stress **A**nalyser **C**ode) [21], a Matlab-based program created by Zanganeh [22] at the University of Sheffield was used to extract fracture parameters from individual displacement field 'frames' produced by the DIC calculations. The technique, algorithms and procedures are documented in [11]. Performing this technique on standard pure-mode I compact tension specimens of the same formulations, and comparing DIC-measured values with values derived by DICITAC, allowed the accuracy of this system to be determined. DIC-measured values were within ±0.05 MPa√m of the 'theoretical' load-cell determined values [23].

In addition to the resin tests, the mode II fracture toughness of carbon-fibre composite specimens was measured. This was achieved by producing unidirectional prepreg on a prepreg tape line using an aerospace-qualified IM fibre using each experimental resin formulation. G_{IIc} values were measured using a variation of the prEN 6034 End Notch Flexure (ENF) method; this method was varied by using a mode II instead of mode I precrack.

Results and discussion

Stress intensity values

K_I and K_{II} values at failure; K_{IQ} and K_{IIQ}, (the subscript Q referring to the value at failure load Q, to avoid confusion with subscript c referring to a material toughness value) were taken immediately prior to fracture and plotted against loading angle for all materials. These are presented in figures 2a-e. These figures show that the data exhibits an approximately linear relationship between 15° and 90° loading, i.e. when $K_{II} > 0$.

Values of K_I/K and K_{II}/K (i.e. normalised for applied stress; K is globally applied stress σ multiplied by $\sqrt{a}$) for angled edge-cracks subjected to tension theoretically follow co-sinusoidal and sinusoidal based relationships respectively as the crack angle varies [24]. However the values at failure do not appear to follow this relationship, nor is there any reason kinking cracks in non-homogeneous materials would be expected to. Linear regression lines have been applied to these data to aid statistical processing.

Investigating the multiple toughening mechanisms of the materials under question, including crazing/microcracking; crack path deviations and bifurcation; toughening agent debonding, cracking, crack bridging and crack pinning; in addition to 'plastic' shear yielding behaviour, leads to the idea that different toughening mechanisms contribute to toughness in different modes differently. There is a strong discontinuity in K_{IQ} behaviour from pure mode I (i.e. K_{Ic}), to the mixed-mode stress intensity factor values (figure 2). The suspected reason for this step-change in behaviour is that as a non-zero shear component is introduced, the fracture behaviours, specifically the active toughening mechanisms, change significantly. All mixed-mode and mode II specimens failed with sudden, kinking cracks. However, the cracks of specimens loaded in pure mode I failed more progressively, without change in crack direction.

Similar behaviour is observed in composite materials; gradual propagation, or sometimes stick-slip crack propagation occurs in mode I G_{IC} DCB specimens, whilst sudden crack propagation occurs in mode II G_{IIc} 3PB-ENF specimens. This idea is discussed in the recent G_{IIc} testing standard ISO15114:2014 [25].

Similar step-like differences in toughness from pure mode I to the mixed-mode region have previously been observed in mixed-mode tests of carbon-epoxy in a study by Reeder [26]. All three of the carbon-epoxy materials tested exhibited an increase in G_{IQ} (G_I at failure) when G_{II} was increased from zero. In the bulk resin specimens presented currently, the step-change for most materials (including the particle untoughened system) can be seen to be a decrease in mode I toughness rather than cause an increase. Thus, there is evidence that there is a step-like disparity between pure mode I behaviour and mixed-mode behaviour in both composite and bulk material.

K_I and K_{II} values measured at the supposedly pure shear conditions of the 90 degree specimens were comparatively more difficult to measure than in the pure mode I and mixed-mode conditions due to relatively small displacements and the presence of tractions on the crack flanks. Indeed, some specimens measured slightly negative mode I components, indicative of crack closure and crack-flank tractions (and non-compliance with the Williams equation boundaries). Consequently, a

method of extracting a mode II fracture toughness from mixed-mode data, rather than relying solely on the 90 degree loading was sought.

Numerous studies have used mixed-mode failure criteria to compare with experimental data. There are many different criteria, however the simplest and most widely used is the Mixed-Mode Failure Envelope (MMFE), equation (2).

$$\left(\frac{K_{I_Q}}{K_{Ic}}\right)^m + \left(\frac{K_{II\,Q}}{K_{IIc}}\right)^n + \left(\frac{K_{III\,Q}}{K_{IIIc}}\right)^o = 1 \qquad (2)$$

The fundamental assumption of the MMFE is that failure occurs at a material critical energy release rate G_c and that the three failure modes each contribute to failure relative to the toughness in the respective mode. Thus, failure can be separated into three commutable proportions of failure, one to each mode. This approach is used as a failure criterion in the widely used Virtual Crack Closure Technique (VCCT) for design of composite components [27].

It is noted that the selection of powers *m*, *n* and *o* using this method is not phenomenonalistic; powers are chosen for their fit.

The previously mentioned study by Reeder [26], in which toughness G_c was observed to increase in carbon-epoxy composites at small, non-zero, levels of K_{II}/K_I, sought to identify the most appropriate failure criteria. A wide range of criteria in the literature were analysed to find which could 'capture' this rise in toughness, in an attempt to fit the entire material behaviour 'curve', from pure mode I to pure mode II, to a semi-analytically derived failure criteria. The approach presented in this paper differs in that instead of attempting to capture the complex 'elbow' curve that fitted through all points would make, the pure mode I behaviour has been analysed separately to the mixed-mode behaviour. As established earlier, the fracture failure mechanism in 'brittle' materials under shear still occurs micromechanically, as a mode I fracture process, albeit after an apparent mode II value has been overcome.

To account for the discrepancy in material behaviour between pure mode I and mixed-mode loading, the value of K_{Ic} in the MMFE was replaced with a mixed-mode effective value. This was defined by extrapolation of the mixed-mode K_{IQ} regression line to the pure mode I, zero degree loading angle case. This is thought to give a failure value that appropriately describes the mode I 'toughness' with regards to the mode I contribution to failure in mixed mode loading. Thus, this value of effective K_{Ic} aims to sum the influence of mode I toughening mechanisms that are 'active' under kinking failure and remove those that do not contribute toward kinking failure, but do contribute toward the more progressive fracture observed in (pure mode I) compact tension tests. It is worth mentioning that the K_{IQ} values at $\phi = 0$, the pure mode I case, were in close agreement with K_{Ic} values as measured using standard, compact tension specimens and the BS ISO 13586 method [28]. Through this modification of the standard MMFE criteria, it was found that despite the non-pure shear failure, this empirical description's envelope closely fitted the material-specific behaviours of our results.

By disregarding the mode III contributions, and using empirically appropriate powers m and n of 1, a value of K_{IIc} can be determined for each specimen tested. At low loading angles, $K_{IIc} >> K_{IIQ}$ which resulted in numerical instability and so only specimens of $\phi \geq 30°$ were considered. Values of apparent K_{IIc} for each material were averaged, and the standard deviation of each set was calculated. These values can be found in table 1.

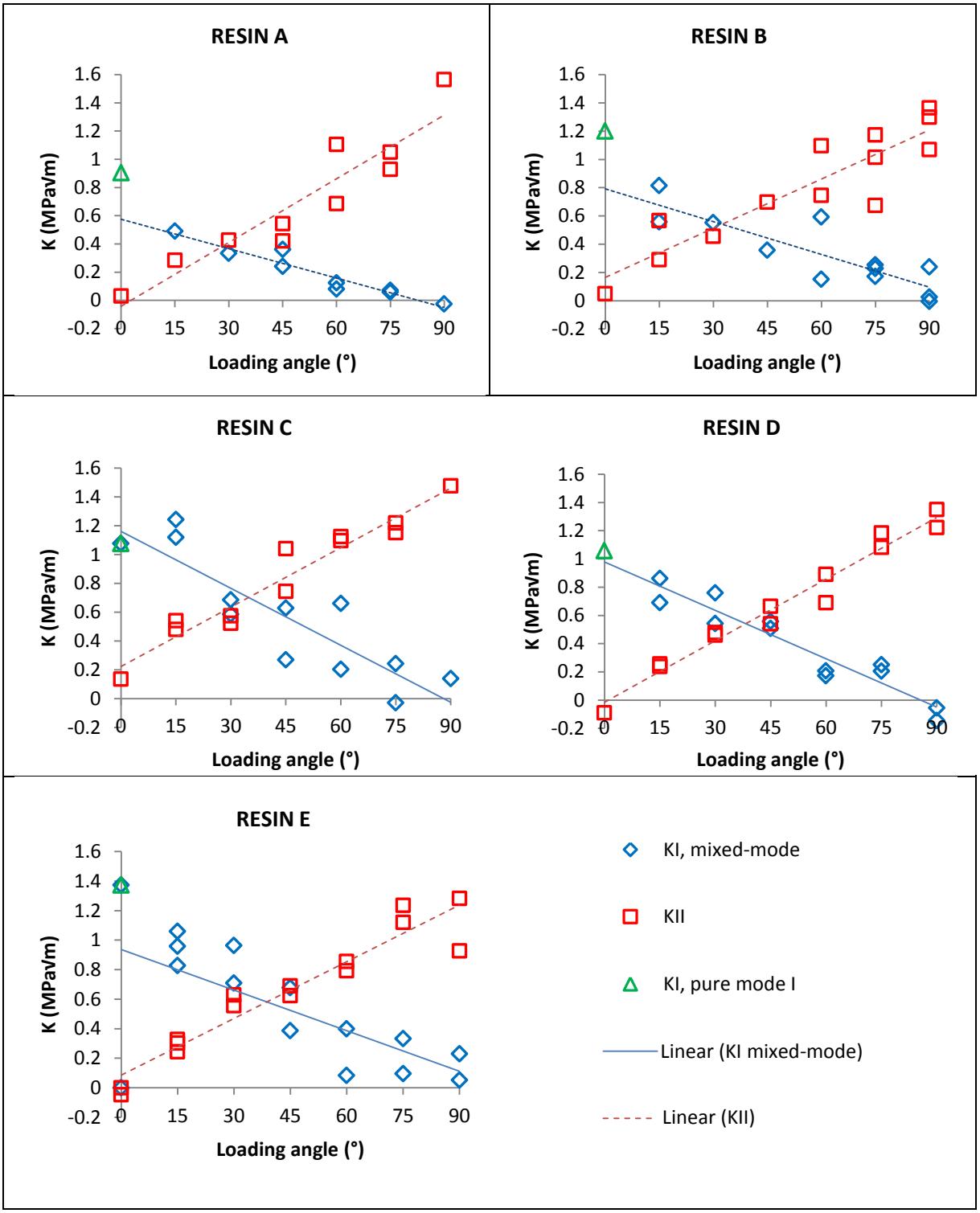

Figure 2 – K_I and K_{II} values at failure

Table 1 – Normalised composite GIIc and measured apparent resin K_{IIc} values.

Material	Composite GIIc (normalised)	Apparent resin K_{IIc} (normalised)	Standard deviation	Coefficient of variance
A	1.00	1.00	0.22	22%
B	1.98	1.17	0.19	16%
C	2.54	1.25	0.30	24%
D	0.89	0.90	0.20	23%
E	1.37	1.09	0.28	26%

Resin K_{IIc} results were compared to composite mode II fracture toughnesses of each formulation (figure 3). The average G_{IIc} value from six to thirteen specimens' average G_{IIc} values are presented. G_{IIc} values have been normalised to the baseline resin 'A'.

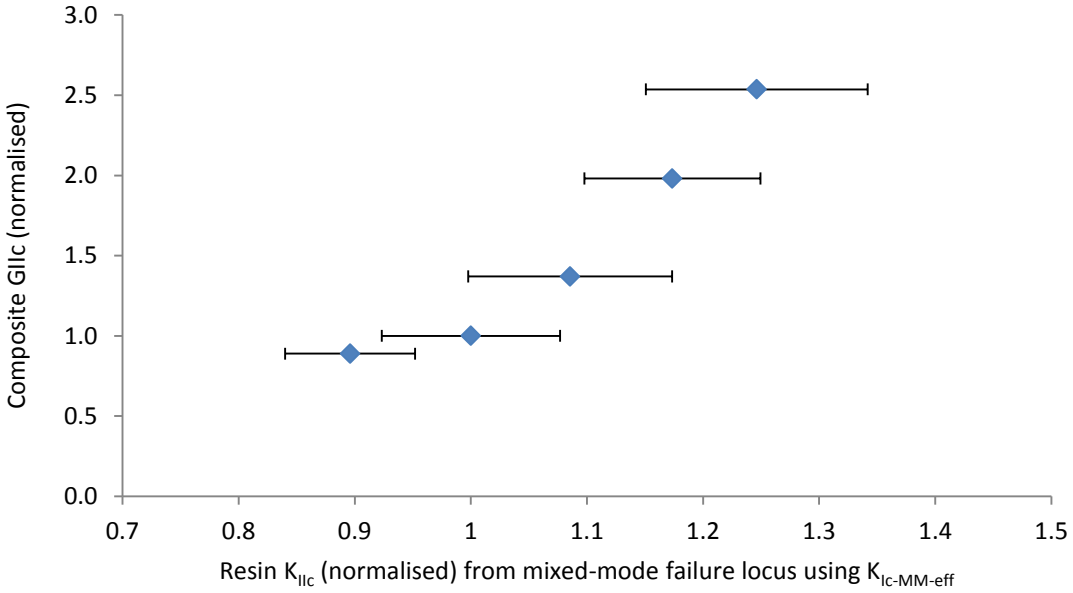

KIIc error bars: $SE\bar{x} = \pm s/\sqrt{n}$

Figure 3 – Resin apparent K_{IIc} against composite G_{IIc} for experimentally toughened systems

Figure 3 suggests that there is a positive correlation between the shear component at fracture in resin, i.e. the normalised resin K_{IIc} using a mixed-mode failure locus, and the composite interlaminar shear behaviour, i.e. G_{IIc}.

In a composite subject to mode II loading there are a multitude of individual 'cracks' resisting mode I growth under shear, as evidenced by the ubiquitous 'shear hackle' of GIIc fracture surfaces. The resin mixed-mode tests presented here describe a method of measuring an apparent resin shear toughness, indicating the resistance of the crack to kinking toward mode I and subsequently propagating. This is thought to be analogous to the micromechanical behaviour of the resistance of individual hackles. Consequently, it is understandable that small differences in 'unconstrained' bulk resin K_{IIc} performance correspond to larger G_{IIc} changes in the composite.

As one continues to increase resin mode I toughness, improvements in composite G_{Ic} are more difficult to realise and the relationship flattens since less benefit can be exploited within the tightly constrained, narrow resin interlaminar layer in a composite [1]. However, for small improvements in the micromechanical mode II resin toughness, the opposite situation appears to occur, and huge improvements in composite G_{IIc} are realised. This is due to the laminate structure constraining the fracture between the plies, allowing toughening effects to occur over a longer distance along the crack-path.

The resin G_{Ic} values calculated in this study are lower than the composite G_{IIc} values. However, this compounds the difficulties in studying mode II performance further; the failure mechanism in both resin shear-loaded fracture and composite G_{IIc} ENF test are already both inherently unstable and both are subject to much scatter. Nevertheless, statistically significant differences in resin shear fracture performance have been measured and these favourably correspond to composite performances.

Conclusions

2D digital image correlation and parameter extraction has been shown to be a useful tool in the analysis of fairly brittle materials such as epoxy. It has been shown that the shear fracture performance of composites can be related to the behaviour of the matrix resin under a shear component. It is hoped that this study can form the basis for showing further links between resin shear fracture behaviour and composite shear fracture behaviour, aiding the understanding and development of new, tougher aerospace materials.

Difficulties in comparing mode II behaviour in resins and mode II behaviour in composites have arisen previously and been blamed on the huge differences in constraint and behaviour between the two systems [6]. The increase in constraint in a composite changes the global behaviour and hugely increases the energy release rate from a bulk, unconstrained state. The results from the five materials presented here suggest that at a local mechanistic level crack behaviour is similar and quantifiable.

It has been shown that performing direct measurements of parameters at failure, rather than relying upon shape-function and load-based methods, offers a promising insight into connecting the material behaviour of matrix and composite.

Acknowledgements

The authors wish to thank Cytec Engineered Materials for their support.

References

1 Altstadt V, Gerth D, Stangle M. Interlaminar crack growth in third-generation thermoset prepreg systems. Polymer. 1993; 34(4): 907-909
2 Tsotsis TK. Interlayer Toughening of Composite Materials. Polymer Composites 2009; 30(1): 70-86
3 Anderson TL. Fracture Mechanics: Fundamentals and Applications. 3rd ed. 2004: CRC Press.
4 Kim J, Baillie C, Poh J, Mai, YW. Fracture toughness of CFRP with modified epoxy resin matrices. Composites Science and Technology 1992; 43(3): 283-297.
5 Piggott MR, Liu K, and Wang J. New experiments suggest that all shear and some tensile failure processes are inappropriate subjects for ASTM standards. In Grant P and Rousseau CQ, Editors. Composite structures: Theory and practice, 2001; ASTM STP 1383. p. 324-333.
6 Ramsteiner F. An approach towards understanding mode II failure of poly(methyl methacrylate). Polymer 1993; 34(2): 312-317
7 Carpinteri A, Valente S, Ferrara G, Melchiorri G. Is mode II fracture energy a real material property? Computers & Structures, 1993; 48(3): 397-413.
8 O'Brien TK. Composite interlaminar shear fracture toughness, GIIc: Shear measurement or sheer myth? ASTM Special Technical Publication, 1998; 1330: 3-18.
9 Cartié DDR, Irving PE. Effect of resin and fibre properties on impact and compression after impact performance of CFRP. Composites Part A: Applied Science and Manufacturing, 2002; 33(4): 483-493.
10 Sutton MA, Orteu J, Schreier H. Image Correlation for Shape, Motion and Deformation Measurements: Basic Concepts, Theory and Applications. 2009: Springer.
11 Zanganeh M, Tomlinson RA, Yates JR. T-stress determination using digital image correlation. in 11th International Congress and Exhibition on Experimental and Applied Mechanics. 2008; Orlando, Florida.
12 Roux S, Hild F. Stress intensity factor measurements from digital image correlation: post-processing and integrated approaches. International Journal of Fracture, 2006; 140(1): 141-157.
13 Kirugulige MS, Tippur HV. Measurement of fracture parameters for a mixed-mode crack driven by stress waves using image correlation technique and high-speed digital photography. Strain, 2009; 45(2): 108-122.
14 Du Y, Díaz FA, Burguete RL, Patterson EA. Evaluation Using Digital Image Correlation of Stress Intensity Factors in an Aerospace Panel. Experimental Mechanics, 2011; 51(1): 45-57.
15 Williams ML. On the stress distribution at the base of a stationary crack. Journal of Applied Mechanics 1957; 24: 109-114.
16 Lopez-Crespo P, Shterenlikht A, Patterson, EA, Yates JR, Withers PJ. The stress intensity of mixed mode cracks determined by digital image correlation. The Journal of Strain Analysis for Engineering Design, 2008; 43(8): 769-780.
17 Nurse AD, and Patterson, EA. Determination of predominantly mode II stress intensity factors from isochromatic data. Fatigue & Fracture of Engineering Materials & Structures, 1993; 16(12): 1339-1354.
18 Hild F, Roux S. Measuring stress intensity factors with a camera: Integrated digital image correlation (I-DIC). Comptes Rendus Mécanique, 2006; 334(1): 8-12.
19 Banks-Sills L, Arcan M, Bui HD. Toward a pure shear specimen for KIIc determination. International Journal of Fracture, 1983; 22(1): R9-R14.
20 Taher ST, Thomsen OT, Dulieu-Barton JM. Bidirectional thermo-mechanical properties of foam core materials using DIC. in Society for Experimental Mechanics - SEM Annual Conference and Exposition on Experimental and Applied Mechanics 2011. 2011. Connecticut, USA.
21 Zanganeh M. DICITAC. 2010, University of Sheffield
22 Zanganeh Gheshlaghi M. Experimental investigation of crack paths, in Mechanical Engineering. 2008, University of Sheffield. PhD.
23 Jones S. An experimental investigation of the fracture behaviour of particulate toughened epoxies. 2013. Dept. of Mechanical Engineering, The University of Sheffield. PhD Thesis

24 Rooke DP, Cartwright DJ. Compendium of stress intensity factors. 1976: Procurement Executive, Ministry of Defence. Her Majesty's Stationary Office, London.
25 British Standards Institution, BS ISO ISO15114:2014, Fibre-reinforced plastic composites-Determination of the mode II fracture resistance for unidirectionally reinforced materials using the calibrated end-loaded split (C-ELS) test and an effective crack length approach. 2014, BSI
26 Reeder J. 3D Mixed-mode delamination fracture criteria – an experimentalist's perspective. NASA. Available online at http://ntrs.nasa.gov/archive/nasa/casi.ntrs.nasa.gov/20060048260.pdf (accessed 18/12/14)
27 Krueger R. The Virtual Crack Closure Technique: History, Approach and Applications. NASA/CR-2002-211628 (2002)
28 British Standards Institution, BS ISO 13586:2000, Plastics. Determinations of fracture toughness (G_{Ic} and K_{Ic}). Linear elastic fracture mechanics (LEFM) approach. 2000, BSI